



Experimental study of simultaneous effects of porous medium and biodiesel application on spray and combustion characteristics of gasoline–biodiesel blends

Mahdi Aboujafari¹ · Mohammad Sadegh Valipour¹ · Alireza Hajjalimohammadi¹ · Amir Hossein Parivar²

Received: 12 October 2023 / Accepted: 7 May 2024 / Published online: 25 May 2024
© Akadémiai Kiadó, Budapest, Hungary 2024

Abstract

Controllability of combustion characteristics in combustion systems, specifically for internal combustion engines, is vital for environmental compliance. This study experimentally investigated the simultaneous effects of the porous medium (PM) application and biodiesel addition on the spray and combustion characteristics of the gasoline–biodiesel blended fuel. A ring-shaped metal PM with 10 or 20 pores per inch pore density (PPI) is installed in a constant-volume combustion chamber for fuel injection through it. Varied blends of gasoline–biodiesel fuel (volume fraction: 5–15%) are tested at three different temperatures (750–1050 K). The results showed that the blended fuel spray interaction with the PM enhanced the fuel dispersion within the combustion chamber. The spray-projected area fraction increased by 4.4% and 28.2%, with the 10 and 20 PPI PM. The porous medium lowered the combustion pressure, temperature, heat release rate, extended ignition delay, and prolonged combustion duration, facilitating homogeneous combustion. The pressure decrease was around 12% and 59%, and the ignition delay increase was 223% and 263% for the 10 and 20 PPI PM. Conversely, biodiesel addition increased the combustion pressure, temperature, and heat release rate while reducing the ignition delay time. While the pressure increase was more than 100%, the PM reduced it by around 50%. The ignition delay reduction was around 50%, but the PM could increase it from 5 to 218%. Therefore, PM and biodiesel applications can be combined to address high emissions of gasoline–biodiesel blended fuel in free-spray combustion and the prolonged ignition delay associated with PM.

Keywords Porous medium · Combustion · Gasoline compression ignition · Biodiesel · Blended fuel

Introduction

Recent assessments have revealed that internal combustion (IC) engines will not be replaced by all-electric vehicles, at least for the heavy vehicle sector, in the coming years, and the transition will require decades [1]. Therefore, enhancing the efficiency of IC engines and reducing their emissions remain top priorities for researchers.

Conventional diesel engines are favorable owing to their simplicity and cost-effectiveness. Compression ignition (CI) engines outperform spark ignition (SI) engines due to their higher compression ratios and the absence of pumping

losses, resulting in lower hydrocarbons (HC) and carbon monoxide (CO) emissions. However, they must contend with higher nitrogen oxide (NO_x) and particulate matter emissions while striving to maintain their efficiency. Recently, gasoline compression ignition (GCI) engines, which utilize gasoline-like fuels in CI engines, have shown promise [2, 3]. Nevertheless, the primary challenge in commercializing GCI engines lies in controlling combustion characteristics and instabilities. Gasoline and gasoline-like fuels exhibit low reactivity and resist autoignition under specific engine loads during compression ignition. Consequently, various methods have been proposed to address combustion instability in GCI engines, including injection strategies, exhaust gas residual (EGR), biodiesel blending, and oxygen content adjustment [4].

Moreover, commercially available gasoline and other low-octane fuels typically possess lower lubricity and viscosity compared to diesel. Therefore, the successful implementation of GCI technology in existing systems optimized for

✉ Mohammad Sadegh Valipour
msvalipour@semnan.ac.ir

¹ Faculty of Mechanical Engineering, Semnan University, Semnan 35131-19111, Iran

² Iran Khodro Powertrain Company, Tehran, Iran

diesel necessitates fuel characteristics improvement. Consequently, several studies have concentrated on enhancing the fuel characteristics through blended fuels [5, 6]. Researchers have also investigated the combined effects of altering fuel octane numbers, variations in air intake conditions, exhaust gas recirculation, and fuel injection pressure [7, 8]. Additionally, researchers have focused on injection quantity and timing, exploring strategies such as double injection, ozone addition coupled with two-stage direct injection, varying injector spray angles, and pilot injection.

Among the mentioned approaches for improving the fuel specifications to yield the desired combustion properties in GCI engines, the biodiesel addition has shown an acceptable performance. Biodiesel is defined as monoalkyl esters of long-chain fatty acids rooted in renewable fatty raw materials. The typical sources of raw materials are vegetable oil, animal oil, waste, and recycled oil [9, 10]. Environmental impacts of the waste cooking oil disposal, resulting in soil contamination, make it a good choice for biodiesel production. Biodiesel of waste cooking oil has similar specifications to diesel. Besides, it has 21–31% by mass of oxygenated compounds in its structure, which promotes complete combustion. It is claimed that biodiesel combustion releases 44% less CO than diesel and contains no aromatic and sulfur compounds [11]. Intensified research has consistently been implemented to optimize biodiesel production methods and produce more cost-effectively [9, 12–14]. To study the performance of biodiesel in improving gasoline characteristics, Thongchai et al. [15] have compared the spray characteristic of gasoline-biodiesel blended fuel (5% biodiesel) with the neat gasoline fuel in a constant-volume combustion chamber (CVCC). They reported that the spray penetration length of the blended fuel was like neat diesel fuel. In their experiments, the higher ambient pressure resulted in the increased spray cone angle of the blended fuel. Duy et al. [16] have also studied the spray characteristics of gasoline-biodiesel blended fuel in a CVCC under GCI engine conditions. They reported that increased biodiesel fraction in the blended fuel results in increased spray penetration length due to the fuel characteristics and the alteration in fuel injection momentum.

Considering the combustion characteristics of gasoline-biodiesel blended. Das et al. [17] studied the performance of a blended fuel with 5% and 20% volume fraction of biodiesel in a CVCC. Their results showed that the addition of biodiesel shortened the ignition delay, which was due to the oxygen content in the biodiesel. In their study, they investigated the effects of the ambient temperature. However, they did not consider the effects of the oxygen concentration on the combustion characteristics, and their experiments were limited to a constant oxygen concentration of 15%. Vu et al. [18] have investigated the ignition and combustion characteristics of the gasoline-biodiesel blend in a CVCC. Their

study included the effects of different ambient conditions (gas density of 5 kg m^{-3} and 15 kg m^{-3} , ambient temperature of 800–1200 K, and oxygen content of 10–21%). They reported that the higher ambient oxygen and temperature could reduce the ignition delay. Their study did not consider the impacts of the biodiesel concentration and was done at a constant biodiesel volume fraction of 20%. Zhong et al. [19] have studied the spray and combustion characteristics of gasoline-hydrogenated catalytic biodiesel (HCB) blended fuel in a CVCC. They considered different ambient temperatures (800–900 K) and oxygen concentration (10–21%). They concluded that the ignition delay declines as the quantity of HCB increases. The ignition delay and flame liftoff length of blended fuel with 50% gasoline and 50% biodiesel were closer to diesel. In another study, Zhong et al. [20] investigated the autoignition characteristics of gasoline-HCB blended fuel at equivalence ratios of 0.5–1.5, temperature of 655–870 K, and pressures of 10 and 15 bar. They presented a simulation model with an acceptable accuracy for predicting the impacts of pressure, blending, and equivalence ratio on the ignition delay time. In a study, Nam et al. [21] have also confirmed that the increase in ambient temperature and growth of biodiesel proportion in the blended fuel reduces the ignition delay time. However, their study was done with a constant equivalence ratio of 0.5.

In addition to the mentioned strategies for controlling combustion instability in GCI engines, previous studies have shown that besides the common applications of the porous medium (PM) such as heat exchangers, cryogenics, thermal insulation, and thermal energy storages [22], its application in combustion systems, such as burners, can yield stable combustion in a wide range of fuel properties and air/fuel ratios [23]. PM applications have also proven beneficial in controlling combustion characteristics in IC engines [24–27]. Higher projected spray area and multi-jet formation after the fuel spray interaction with the PM result in better air entrainment and air–fuel mixture homogenization [28, 29]. Numerical studies have primarily centered on the heat storage capacity of PM and its impact on combustion zone temperature [30, 31]. Liu et al. [32] proposed a two-zone model, establishing that the delay in diesel ignition in PM depends on the initial PM temperature. Mohammadi et al. [33] conducted a numerical study, revealing that the direct methane injection into PM led to homogeneous mixture formation and a 30% reduction in CO emissions. Certain numerical studies have indicated that PM could significantly reduce NO_x emissions in PM-equipped engines.

Ehyaei et al. [34] have reported that engine efficiency increases by benefiting the PM heat recovery in the combustion process of a typical engine. Cypris et al. [35] utilized an electrically heated constant-volume PM reactor and injected diesel fuel into it for compression ignition. They argued that the combustion pressure peak was lower because of the

decrease in combustion temperature, which resulted from heat storage in the PM. Therefore, a lower amount of NO_x was expected. Experimental investigations on real engines have also shown the positive role of PM in decreasing emissions. Some studies have reported a 70% decrease in CO and HC emissions, a 27% decline in fuel consumption, and insignificant growth in NO_x emission with porous media in the air manifold of the Otto engine [36]. In an investigation, installing the PM in the piston region of a diesel engine has resulted in a decrease in combustion pressure alongside a thermal efficiency decrease of around 20% and NO_x emissions reduction [37]. Another experiment with the PM in the piston bowl showed a considerable decline in the average peak cylinder temperature and pressure. Besides, applying PM with Al_2O_3 and ZrO_2 materials results in a higher ignition delay than SiC PM [38]. The fuel spray interaction with PM can enhance the fuel–air mixture formation and homogenization in the combustion chamber [39, 40]. Some experiments have aimed to deepen the understanding of this issue. Sohrabiasl et al. [41] proposed using metal PM for fuel spray interaction. They reported that the axis line of spray was moved upward after interaction with metal PM, and the PM with higher pore density showed significant signs of fuel rebound from the PM. They didn't test the performance of the metal PM in the combustion process. Shahangian et al. [42] conducted an experimental study on diesel combustion in the presence of a ceramic PM and found that the maximum combustion pressure was lower with PM. They didn't consider the effects of ambient oxygen on the combustion characteristics. Some experimental studies of the spray interaction with the PM have shown that PM porosity plays a critical role in spray formation structure after interaction with the PM [28, 43]. Thermodynamic modeling studies have also demonstrated that the peak temperature in

a combustion chamber filled with PM is decreased with the reduction in the PM pores diameter [44]. Another significant PM characteristic in the fuel spray formation process is its permeability. Permeability is a measure of the frictional resistance of the medium to fluid flow or, in other terms, the drag force of the fluid on the material. When the PM porosity decreases, its tortuosity and specific surface area increase, resulting in reduced permeability [39, 45].

This study's primary goal is to offer benefits from the combined effects of PM application and the addition of biodiesel to gasoline for controlling the fuel compression ignition in GCI engines, substituting the already suggested intricate strategies. In unique experiments, with the presence of a metal (nickel) PM with pores density of 10 and 20 pores per inch (PPI), the combustion characteristics of gasoline–biodiesel fuel blends containing a 5–15% volume fraction of biodiesel were investigated. The material of the selected PM is metallic to eliminate the disadvantages of the ceramic foams, such as low porosity and closed pores, which were used in previous studies. Key parameters were measured, including fuel spray-projected area, combustion pressure rise, temperature rise, ignition delay, and heat release pattern. These properties are critical for combustion and emission control, particularly in GCI engines.

A summary of the most relevant studies available in the literature is presented in Tables 1 and 2.

Experimental setup and methodology

Experimental setup

This study utilized a cylindrical steel vessel (CVCC) with a diameter and length of 135 mm and a volume of 1.7 L to

Table 1 Summary of the studies on the gasoline-biodiesel blended fuel performance in GCI combustion mode

Author(s)	Research type	Main findings
Khoa et al. [4]	Experimental	Gasoline-biodiesel blended fuel increased the combustion stability in GCI engines
Peng et al. [5]	Experimental	Port fuel injection/direct injection strategy with EGR could reduce NO_x with the most negligible side effects
Singh et al. [6]	Experimental	Using blended fuel increased engine performance and decreased emissions
Jiang et al. [7]	Experimental	The GCI engine showed superior performance using gasoline with a research octane number of 70 and heating the intake air
Jiang et al. [8]	Experimental	EGR can significantly lower the GCI engine NO_x emissions
Thongchai et al. [15]	Experimental	The spray penetration length of the gasoline-biodiesel blended fuel with 5% biodiesel was like neat diesel fuel
Duy et al. [16]	Experimental	Increasing biodiesel fraction in the gasoline-biodiesel blended fuel resulted in increased spray penetration
Das et al. [17]	Experimental	The addition of biodiesel reduced the ignition delay of gasoline compression ignition
Vu et al. [18]	Experimental	Higher ambient oxygen and temperature reduced the ignition delay of gasoline-biodiesel blended fuel
Zhong et al. [19]	Experimental	Ignition delay decreases as the quantity of biodiesel increases in the gasoline-biodiesel blended fuel
Nam et al. [21]	Experimental	Increased ambient temperature and biodiesel proportion in the blended fuel reduced the ignition delay time

Table 2 Summary of the studies on the PM application in the fuel spray and combustion processes

Author(s)	Research type	Main findings
Shahangian et al. [28]	Experimental	The fuel spray interaction with the PM resulted in better air entrainment and air–fuel mixture homogenization
Zhou et al. [30]	Numerical	PM application resulted in homogeneous combustion and controlled temperature in the combustion chamber
Sharma et al. [31]	Numerical	The PM application reduced the peak temperature and pressure in IC engines
Liu et al. [32]	Numerical	The ignition timing in the PM of an IC engine equipped with PM depended primarily on the initial PM temperature
Mohammadi et al. [33]	Numerical	The PM reduced the CO emissions in an IC engine fueled by Methane
Ehyaie et al. [34]	Numerical	PM could store the heat of the exhaust gas of an IC engine and reuse the heat to expedite the liquid fuel evaporation
Cypris et al. [35]	Experimental	Applying the PM in a combustion chamber reduced the combustion peak pressure
Tangestani et al. [36]	Experimental	The PM in the air manifold of an Otto engine reduced CO, CO ₂ , HC emissions, and fuel consumption and increased NO _x
Saravanan et al. [37]	Experimental	The engine efficiency decreased by around 20%, and NO _x emissions were reduced by installing the PM in the piston
Das et al. [38]	Experimental	Peak cylinder temperature and pressure by installing the PM in the piston
Dong et al. [39]	Numerical	PM application enhanced the formation of fuel–air mixtures and homogenization in the combustion chamber
Zhao et al. [40]	Numerical	PM application increased the homogenization of the fuel–air mixtures in the combustion chamber
Sohrabiasl et al. [41]	Experimental	The PM with high pore density showed significant signs of fuel rebound from the PM when the spray interacted with it
Shahangian et al. [42]	Experimental	Applying the PM in a CVCC reduced the maximum combustion pressure
Shahangian et al. [43]	Experimental	PM porosity had a significant role in spray formation structure after interaction with the PM
Saghaei et al. [44]	Numerical	Peak temperature in a combustion chamber filled with PM decreased with the reduction in the diameter of the PM pores

investigate the spray and combustion characteristics of the blended fuel for the GCI concept. The PM pieces used had pore densities of 10 and 20 PPI and were manufactured from nickel. They were produced by directional metal solidification from a superheated liquid state under an overpressure and high vacuum environment. The PM produced with this technique has high porosity (almost 90%) and a highly open cell structure, which is appropriate for application in the spray process of IC engines. The ring-shaped PM had a diameter of 60 mm, thickness of 10 mm, and height of 20 mm. Figure 1 provides an illustrative representation of the CVCC and the PM position in the CVCC, and Fig. 2 shows an overview of the experimental setup.

Table 3 lists the fuel specifications. The biodiesel in this study was produced using a transesterification technique from the waste cooking oil (WCO).

A preheating combustion process provided the required temperature and pressure conditions for the main fuel (blended fuel) compression ignition. During the mixture preparation phase of the preheating combustion event, electrical heater elements were employed to elevate the temperature of the gas mixture confined within the CVCC. The initial gas temperature was accurately monitored using a type-K thermocouple, and the initial gas pressure was measured utilizing an absolute pressure sensor. A vacuum

pump removed the air inside the CVCC before the mixture preparation. The gas pressure fluctuations within the CVCC during and after combustion events were monitored using an AVL piezoelectric transducer, type GU12P, with less than 0.3% linearity error (piezoelectric sensors are very stable in their long lifetime). The calibration of the pressure sensor was checked by a Druck company pressure calibrator. The pressure was recorded with an AVL INDISET 620 data acquisition unit, featuring a time resolution of 0.01 ms. The fuel was injected into the CVCC by a high-pressure injector equipped with eight sac-hole nozzles featuring a 0.12-mm orifice.

The CVCC was designed with two glasses to facilitate optical observations. The cold spray (non-combusting) injection process was captured using a Motion Blitz CUBE3 high-speed camera (maximum resolution: 512 × 512 at 2500 fps) using the Schlieren technique. Images were captured at a speed of 13,632 fps and a resolution of 160 × 94 pixels.

Experiment conditions and procedure

For the cold spray tests, high-pressure fuel injection was conducted through the PM to assess the impacts of the PM on the blended fuel spray characteristics. The chamber pressure was maintained at 1 atm. The high-speed camera

Fig. 1 **a** Photograph of the CVCC, **b** photograph showing the position of PM in the CVCC, and images showing the shape of **c** PM10 and **d** PM20

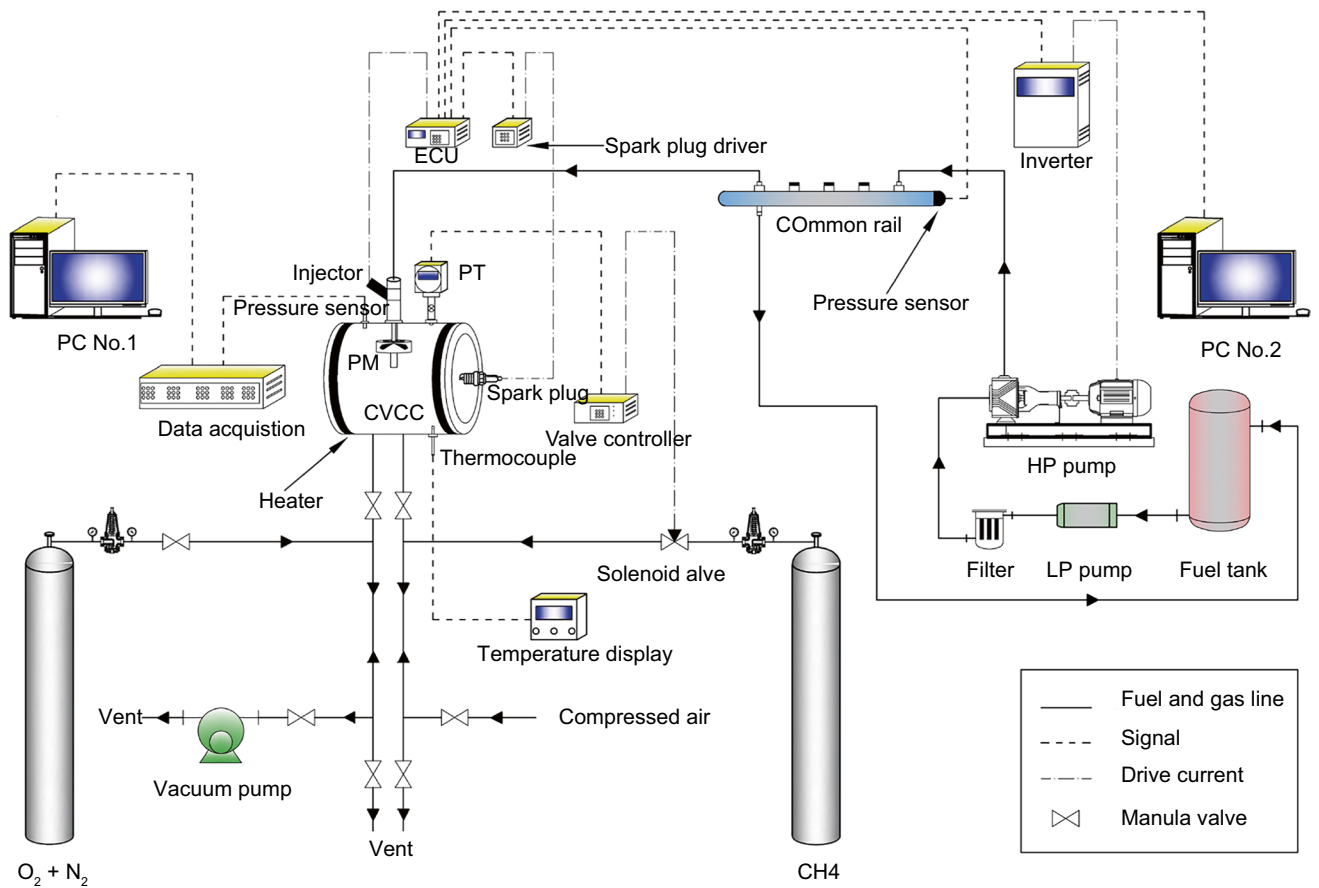
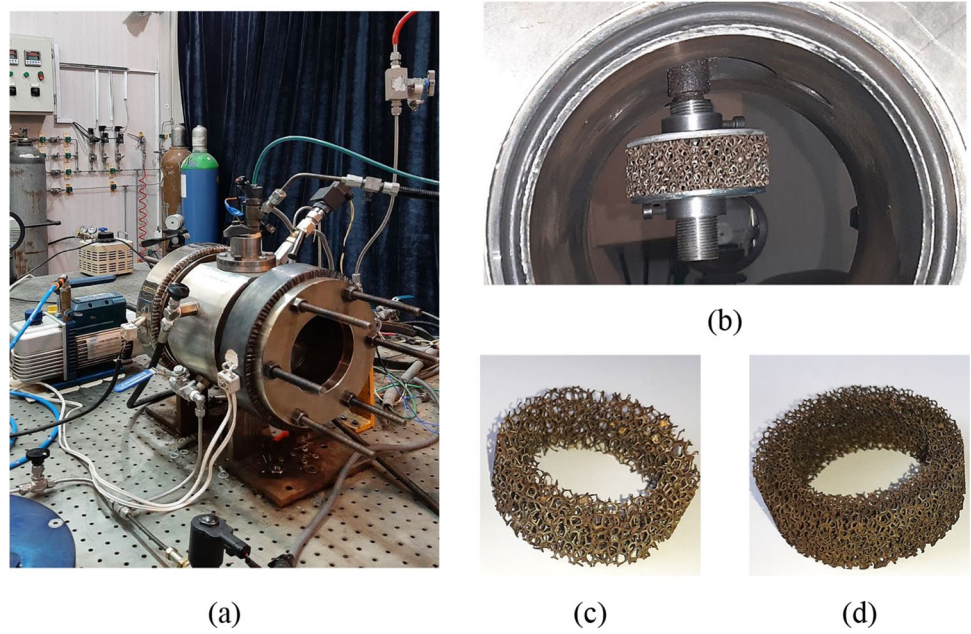


Fig. 2 Schematic of the experimental setup for combustion tests

Table 3 Specifications of fuels

Property	Testing standard	Unit	Value	
			Gasoline	Biodiesel
Density	ASTM D4052	g mL ⁻¹	0.760	0.874
Low Heating Value	ASTM D240	MJ Kg ⁻¹	43.65	41.97
Sulfur Content	ASTM D5453	PPM	18.4	15
Water & Sediment	ASTM D2709	vol%	–	<0.01
Water Content	ASTM D6304	PPM	95	–

recorded the fuel injection process, and MATLAB codes were prepared to analyze the resulting images using image processing techniques.

In the combustion tests, the pressure and heat required for fuel compression ignition of the fuel (engine-like conditions) were generated through the combustion of natural gas with the appropriate excess air. The preheating mixture with a density of 3.5 kg m⁻³ was prepared by the partial pressure measurement of the natural gas and a synthetic air made of 50% volume O₂ and 50% volume N₂ in the CVCC. Subsequently, the mixture was ignited by a spark plug. The amount of air was adjusted to ensure the necessary oxygen content remained after the combustion of the preheating mixture for the primary fuel (gasoline and biodiesel) combustion. EGR was simulated by modifying the O₂ volume to 15%. The fuel injection pressure, a determining factor in the fuel spray formation, was adjusted to 600 bar to ensure the gasoline compression ignition occurrence [19]. The tests were conducted at three different temperatures at which the fuel injection was started (SOI), namely T_1 , T_2 , and T_3 . The temperature range was selected as it falls within the low-temperature combustion (LTC) range. LTC encompasses the combustion process at a lower temperature and sufficiently lean to avoid the high NO_x and soot formation zones in CI engines [18, 46]. Considering the results of previous experimental studies, the PM pore density, which significantly impacts the PM's spray formation and heat storage capacity, was defined as 10 and 20 PPI to meet the PM application requirements in the IC engines' combustion process [27, 42]. Since this study intended to investigate the strategies for aiding the gasoline compression ignition in GCI engines, the added biodiesel fraction to the blended fuel was 5–15%. This amount of biodiesel was sufficient to significantly impact the fuel properties, such as lubricity, and combustion behavior, such as ignition delay time [17]. The test conditions are summarized in Table 4.

Considering that the gas inside the CVCC is ideal and that combustion occurs as a constant-volume process, the heat release rate (HRR) can be correlated with the gas pressure using the first law of thermodynamics as described by Eq. (1) [42], and the heat transfer to the chamber wall as a

Table 4 Test condition for the combusting fuel spray tests

Property	Quantity
Ambient temperature/K	$T_1 \approx 750$, $T_2 \approx 900$, $T_3 \approx 1050$
Injection pressure/bar	600
Injection duration/ μ s	2000
PM pore density/PPI	10, 20
Biodiesel volume fraction/%	0, 5, 10, 15

function of the gas temperature inside the CVCC is estimated using Eq. (2).

$$\frac{dQ_n}{dt} = \frac{dQ_g}{dt} - \frac{dQ_{ht}}{dt} = \frac{1}{\gamma - 1} V \frac{dP}{dt} \quad (1)$$

$$\frac{dQ_{ht}}{dt} = Ae^{BT} \quad (2)$$

In Eqs. (1) and (2), Q_n is the net heat release (NHR), calculated by measuring the CVCC pressure variation over time. Q_g is gross heat release (GHR—energy released by the fuel combustion), which is calculated by subtracting the heat transfer to the CVCC wall from the net heat release, $\gamma = c_p/c_v$, Q_{ht} is the heat transfer from the CVCC to the ambient through the chamber walls, and V is the CVCC volume. The heat transfer to the CVCC wall exists all the time, including during the precombustion and primary combustion, and is mainly a function of the gas temperature inside the CVCC, temperature of the CVCC wall, and ambient temperature. Therefore, in this work, the heat transfer to the chamber wall was assessed by fitting an exponential function of gas temperature by utilizing the data of the gas temperature decrease due to the heat transfer to the CVCC wall before the main combustion event. Consequently, the gross heat release rate (GHRR) is calculated with Eq. (3) yielded by summing the net heat release rate (NHRR), which is obtained by measuring the CVCC pressure fluctuations (dP/dt in Eq. 1) and calculating the CVCC heat transfer rate (Eq. 2). As mentioned earlier, since the heat transfer rate is a function of the gas temperature inside the CVCC, it is calculated individually for each condition of the designed experiments.

$$\text{GHRR} = \frac{dQ_g}{dt} = \frac{dQ_n}{dt} + \frac{dQ_{ht}}{dt} \quad (3)$$

The three primary sources of uncertainty in these measurements are the repeatability of the preheating gas mixture combination, the opening behavior of the fuel injector needle, and the unpredictable turbulent behavior of the fuel spray. Five tests were performed under the same experimental conditions to validate the repeatability of the test

results. The uncertainty of the experiments was calculated for a confidence level of 95% with Eq. (4), where t_s is the Student's distribution factor, σ is the standard deviation, N is the number of tests, and x_m represents the mean value of the measurements [47]. The results yielded a standard deviation of 0.06 and an uncertainty of 7.9% for the maximum pressure rise.

$$Un(\%) = \frac{t_s \sigma}{\sqrt{N}} / x_m \tag{4}$$

Results and discussion

Effects of the PM on the blended fuel spray

The spray-projected area is a crucial parameter in fuel atomization, significantly influencing air–fuel mixing quality, a prerequisite for efficient air entrainment. A larger spray area implies a greater portion of the injected fuel coming into contact with the surrounding air, leading to accelerated evaporation of fuel droplets within the combustion chamber [48]. Figure 3 illustrates the penetration of the GB10 blended fuel spray into the combustion chamber over time. The fuel-rich core of the spray remains close to the PM even after 3.5 ms for PM20, indicating more pressure loss compared to the PM10 scenario. Signs of the multi-jet splitting effect on the fuel spray emphasized by Weclas et al. [49] were observed for PM10 when $t=0.4$ ms.

Figure 4 presents the projected spray area fraction of the total combustion chamber space covered by the projected spray area when the spray reached the end wall of the combustion chamber computed by image processing

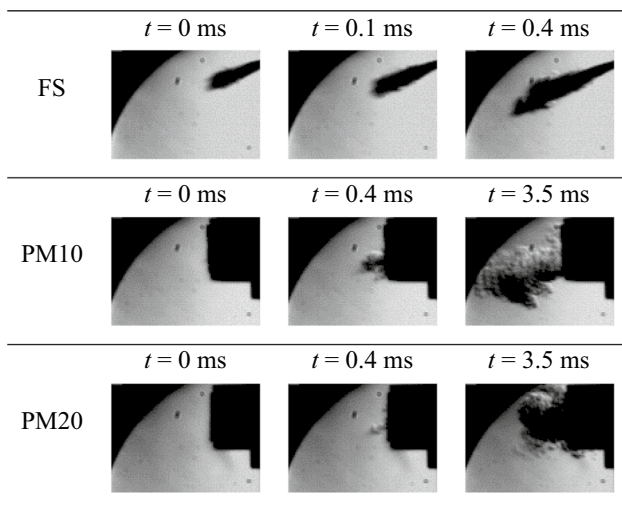


Fig. 3 Free spray of GB10 and its interaction with PM over time

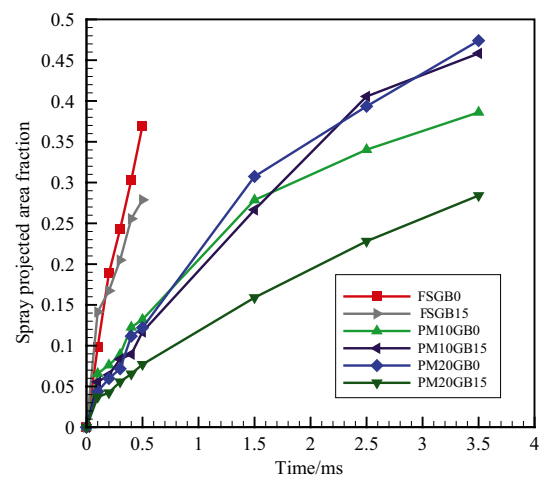


Fig. 4 Variation in the spray-projected area fraction of different fuels with time

techniques and writing a code in MATLAB [50]. The free spray reaches the end wall within a mere 0.5 ms, while the fuel requires 3.5 ms for the PM case to reach the end wall. Biodiesel fuels have higher density, viscosity, and surface tension values than gasoline and diesel. Thus, with the addition of biodiesel to gasoline fuel, the fuel viscosity and density increase. The rise in the viscosity and surface tension of the fuel will increase the spray penetration length due to resistance against break up. The higher density also causes higher momentum flux and promotes higher penetration length. However, the higher viscosity and density increase the internal losses in the fuel injector and impose a delay in the start time of fuel exit from the injector tip. This delay in the injection start causes the gasoline to have greater penetration at the beginning of the injection. After a definite time, blended fuel will have a higher penetration rate. Comparing the PM cases reveals that the fuel dispersion within the space for PM10 is more than that for PM20 at 1 ms, but PM20 disperses the fuel in the combustion chamber space more than PM10. The projected spray area for the blended fuel is lower than that of pure gasoline in the free-spray scenario, a consequence of less effective spray breakup, which is consistent with the results reported in previous studies [51]. Although the PM application extended the projected area, the higher viscosity and density of the blended fuel had a detrimental impact on PM performance, particularly in the case of higher pore densities. For example, the final spray-projected area for the PM20 with a 15% biodiesel volume fraction is almost equal to that of free spray with the same quantity of biodiesel.

Effects of the PM on the blended fuel combustion characteristics

Pressure and temperature rise

The combustion chamber pressure and temperature variations during the free spray of the gasoline–biodiesel fuel blend at three different SOI temperatures are shown in Fig. 5. Notably, as the biodiesel volume fraction increased, the pressure and temperature in the combustion chamber increased significantly. However, as temperature increased with the augmentation of the biodiesel volume fraction, the differences in pressure and temperature growth became less pronounced. The gas pressure rises higher at lower temperatures. This increase in pressure is primarily attributed to longer ignition delays at lower temperatures, leading to more extensive premixed combustion and a higher chamber pressure. Reduced emissions of CO, HC, and particulate matter are expected when using biodiesel. However, the NO_x formation is enhanced due to the increased oxygen content in the fuel and high combustion temperature. Notably, the actual flame temperature of biodiesel may exceed that of fossil fuels. This effect is attributed to lower radiative heat transfer from soot through the flame, as biodiesel combustion generates less particulate matter [52].

Figure 6 depicts the effects of adding biodiesel to gasoline on the temperature and pressure in the presence of PM. Even with applying PM, the pressure and temperature increased with the addition of biodiesel. Compared with the free-spray cases, PM application almost entirely compensated for the consequences of biodiesel addition. The maximum temperature for the free spray with 15% volume of biodiesel was approximately 180 K, whereas the maximum temperature was approximately 120 K for PM20. The performance of PM in the combustion peak temperature reduction is a good substitute for high levels of EGR in CI engines, which has the intrinsic consequences of high CO emissions and decreased fuel conversion efficiency.

Heat release

Figure 7 presents the fuel's GHRR (gross heat release rate) and GHR (gross heat release). The GHRR peak of the blended fuel is significantly higher than that of pure gasoline. For example, the maximum GHRR at the temperature of T_3 is 0.18 kJ ms^{-1} for the free-spray case, whereas the maximum GHRR is 0.31 kJ ms^{-1} for the GB10 blended fuel. The difference between the peak GHRR diminishes as the temperature increases, and the GHR of the blended fuel is greater than that of pure gasoline.

When the biodiesel volume fraction increases, some factors affect the higher heat release rate. Increasing the

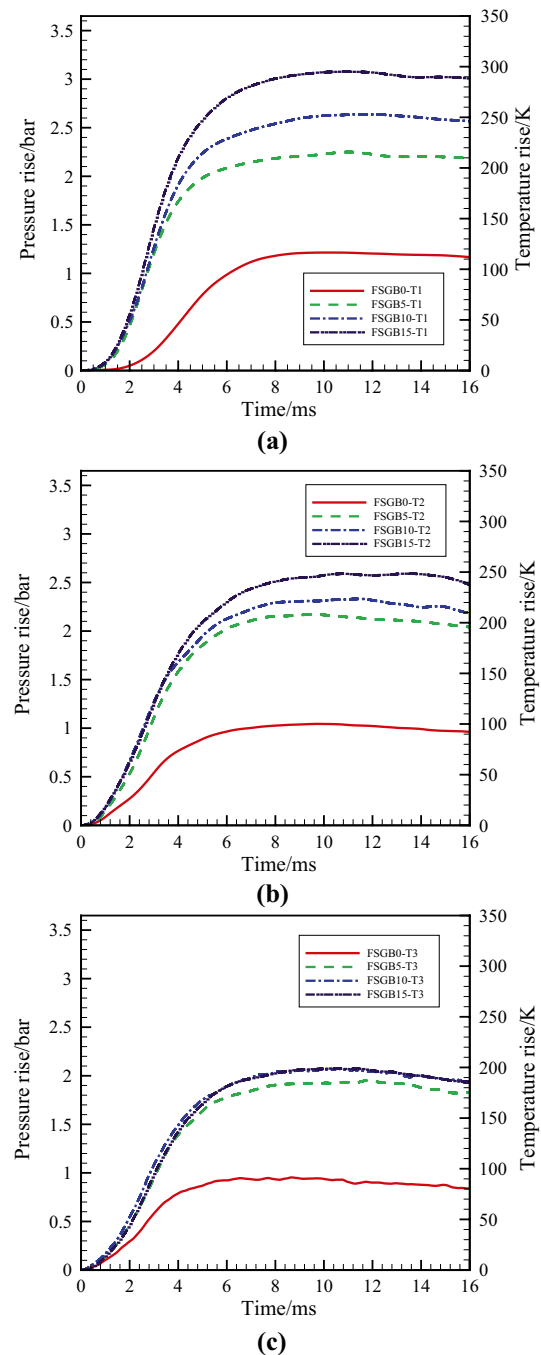
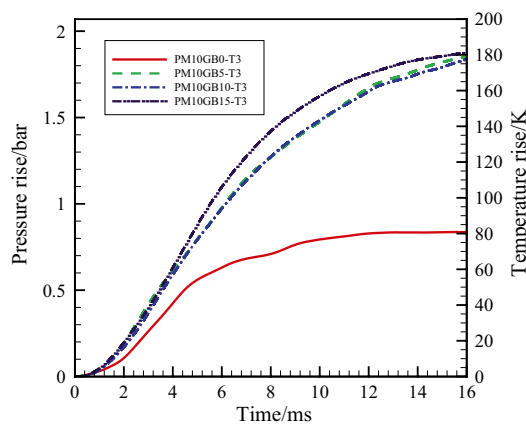
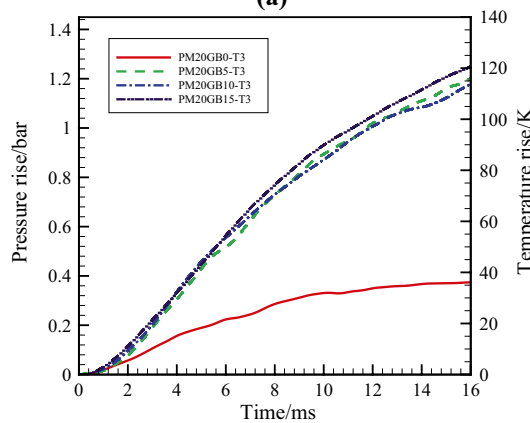


Fig. 5 Effects of biodiesel addition on combustion pressure and temperature at different SOI temperatures: **a** T_1 , **b** T_2 , and **c** T_3

biodiesel volume fraction enhances the blended fuel density, resulting in a higher initial injector needle lift. Therefore, although the blended fuel spray breakup is weaker than pure gasoline, pure gasoline's initial mass flow rate is less than that of blended fuel. Therefore, the fraction of fuel burned in the premixed combustion phase is higher for blended fuel. The higher quantity of the fuel burned in



(a)

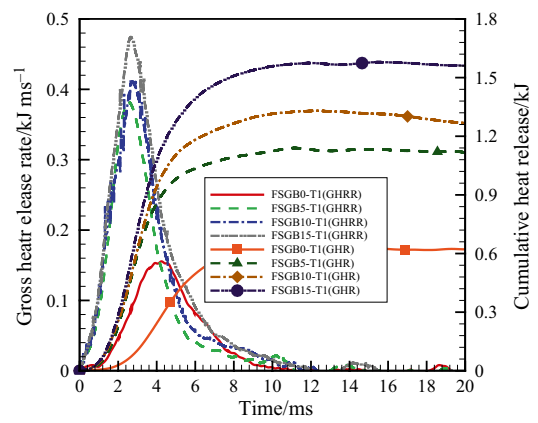


(b)

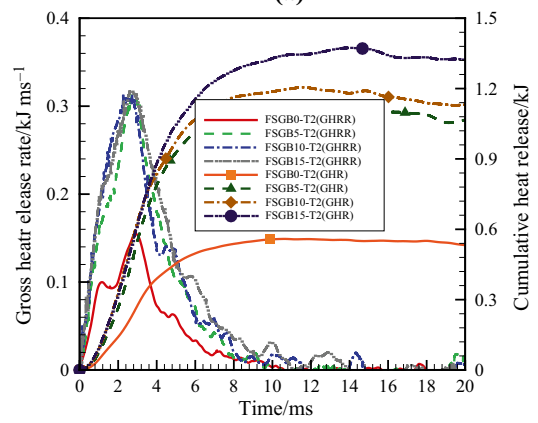
Fig. 6 Effects of biodiesel addition on combustion pressure and temperature increase in PM presence: **a** PM10 and **b** PM20

premixed combustion mode and the oxygen in the blended fuel result in a higher fuel heat release. The impact of premixed combustion on heat release regarding the SOI temperature is also evident for blended fuel; as the SOI temperature increases, the ignition delay decreases, less premixed combustion dominates, and therefore, the peak heat release is lower for T_3 than T_1 .

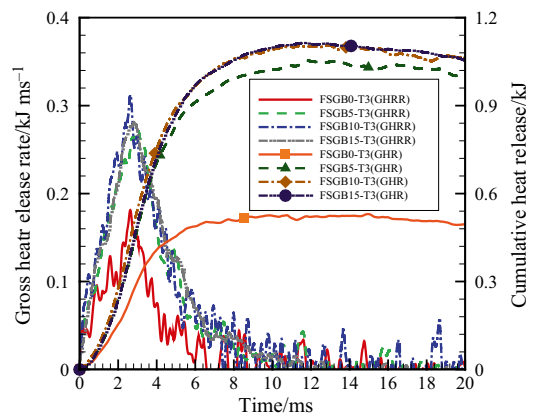
Figure 8 displays the GHRR and GHR of the fuel blended with PM. PM continues to play a pivotal role in extending the GHRR. However, for the blended fuel, the rate substantially increased. Although the maximum GHRR of pure gasoline is approximately 0.08 kJ s^{-1} for PM10 and 0.03 kJ s^{-1} for PM20, with GB10, the corresponding values are 0.11 and 0.07, respectively. Considering the impact of the PM pore density, it is observed that a higher amount of heat absorption relative to the free-spray and PM10 cases occurs in the case of PM20, which results from the higher heat storage capacity. The extended heat release for PM20 implies the combustion continuation in the broader volume of space and



(a)



(b)



(c)

Fig. 7 Effects of biodiesel addition on heat release at different SOI temperatures: **a** T_1 , **b** T_2 , and **c** T_3

within the PM structure, in addition to a gradual release of stored heat by the PM. This extended heat release results in a more homogenous temperature distribution in the combustion chamber, which is essential for the LTC concept.

Figure 9 illustrates the blended fuel's net heat release (NHR). The NHR increased significantly when the biodiesel

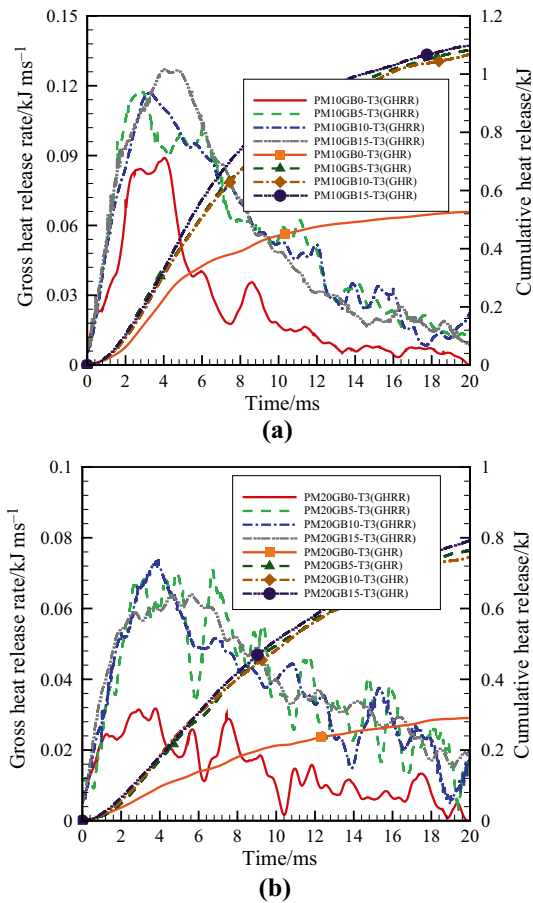


Fig. 8 Effects of biodiesel addition on gross heat release in PM presence: **a** PM10 and **b** PM20

volume fraction increased. Moreover, the difference between the NHR of the blended fuels decreased as the biodiesel fraction increased. For instance, for the PM10 case, although the NHR peak for GB5 was 131% higher than GB0, for GB15, the maximum NHR was only 3.1% higher than that for GB10.

Ignition delay time

The current study defines the ignition delay time as the interval between the fuel injection's start and the CVCC pressure rise due to fuel ignition. Figure 10a plots the computed ignition delays of pure gasoline with the presence of the PM at three SOI temperatures. The pre-ignition reaction rate accelerates as the temperature increases, decreasing ignition delay time. PM application notably influences ignition delay growth, which is significantly higher at lower temperatures. As the PM pore density increases, the ignition delay increases owing to the delay in spray penetration in the combustion chamber, showing the impact of the PM structure properties on the combustion. This

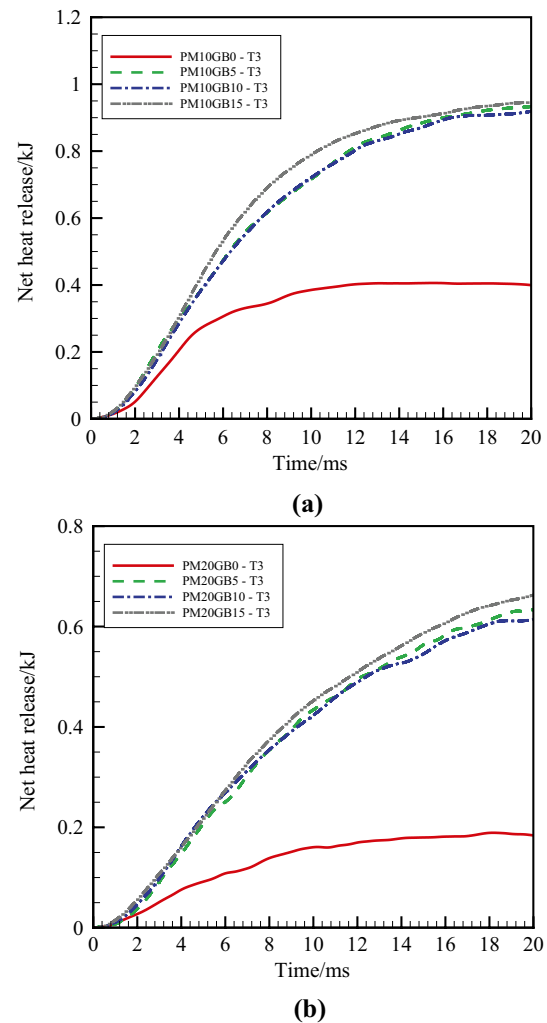


Fig. 9 Effects of biodiesel addition on net heat release in PM presence: **a** PM10 and **b** PM20

trend indicates that combustion does not occur in the PM structure at low temperatures. The non-occurrence of fuel combustion in the PM complies with the numerical study of Zhao [22], which deduced that the compression ignition in the PM structure does not occur at a temperature below 1000 K. However, as the PM pore density increases at high temperatures, the expedited air–fuel mixture preparation process, including vaporization, significantly impacts the ignition delay time owing to the higher heat capacity of the PM. The ignition delay is a strong function of the PM structure's temperature and fuel properties. Thus, higher PM structure temperatures can reduce ignition delay by expediting fuel evaporation.

Figure 10b plots the ignition delay times for the free-spray and PM cases with biodiesel addition. Gasoline has a high resistance to autoignition, and as expected, the addition of biodiesel shortens the ignition delay time. In particular, the biodiesel's oxygen content and the fuel's cetane

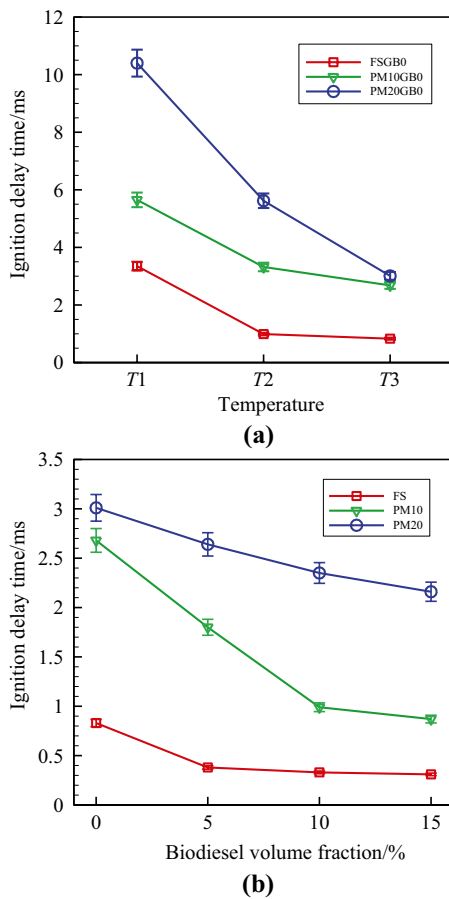


Fig. 10 Effects of PM on ignition delay time: **a** pure gasoline at different SOI temperatures and **b** blended fuel at T_3

augmentation were the main factors responsible for the decrease in ignition delay. For the free-spray case, adding 5% biodiesel to gasoline significantly affected the ignition delay time, and the ignition delay times for adding 10% and 15% biodiesel were approximate to that for 5% biodiesel. Furthermore, adding biodiesel from 5 to 15% PM significantly reduced the ignition delay.

Lengthier ignition delay due to applying PM can provide enough time for the mixture preparation process, which is crucial for LTC combustion. By using metal PMs such as nickel foams used in this study, it is possible to control the ignition delay time mostly and impose the desired combustion characteristics such as ignition delay time and lean combustion occurrence by electrical heating of the PM. Besides that, the nickel PM has good electrical conductance and heat transfer properties, guaranteeing a uniform PM structure temperature. It presented good mechanical resistance under high-pressure and temperature conditions during the tests of this work and showed no sign of failure.

Comparing the effects of the PM application on the blended fuel combustion

Considering the effects of PM application and biodiesel addition on the combustion characteristics, Table 5 shows the quantities of the pressure rise and ignition delay time (the ignition delay time is assumed for an engine with a rotational speed of 1000 RPM) in different cases and compares them with those of the free-spray cases. Considering the increments in combustion pressure and temperature, the PM had diminished the effects of biodiesel addition remarkably. For instance, while a 15% volume fraction of biodiesel addition had resulted in a 118% pressure increase in the free-spray case, the pressure increase by application of PM20 is around 52%. The PM also significantly influences the ignition delay time. For example, while the decrease in the ignition delay time due to a 15% volume fraction of biodiesel addition was approximately 63%, the ignition delay time increased only 5% by application of PM10, which implies that the PM has compensated the effects of the biodiesel addition on the ignition delay time. Therefore, considering specific solutions proposed in the literature to overcome the emission and performance criteria for GCI engines, the combined effects of PM and biodiesel should be regarded seriously.

Table 5 Effects of PM application on combustion characteristics of blended fuel

Characteristics	Case	Biodiesel volume fraction							
		0%		5%		10%		15%	
		Quantity	Variation/%	Quantity	Variation/%	Quantity	Variation/%	Quantity	Variation/%
Pressure rise/bar	FS	0.952	–	1.952	105	2.074	118	2.077	118
	PM10	0.836	–12	1.931	103	1.917	101	1.976	107
	PM20	0.389	–59	1.417	49	1.376	44	1.444	52
Ignition delay/ crank angle degree	FS	4.98	–	2.28	–54	1.98	–60	1.86	–63
	PM10	16.08	223	10.8	117	5.94	19	5.22	5
	PM20	18.06	263	15.84	218	14.1	183	12.96	160

Conclusions

This study investigated the effects of PM application in the fuel injection process and biodiesel addition to gasoline on fuel spray evolution and compression ignition at different temperatures. The main aim of this research was to recommend ideas to tackle the challenges in gasoline compression ignition to expedite the development of GCI engines, which are more efficient and environmentally friendly than conventional IC engines. The results revealed interesting trends and findings regarding the maximum pressure and temperature rise, ignition delay time, gross heat release rate, and cumulative gross heat release. The significant findings of this study are summarized as follows.

1. The SOI temperature significantly affects the heat release of the blended gasoline–biodiesel fuel. In lower temperatures, the peak heat release is higher. When the temperature increases, the difference between the heat release of the blended fuels with different biodiesel fractions diminishes.
2. Although PM application delays the entrance of the fuel into the combustion chamber, the interaction of the fuel spray with the PM structure yields a better air–fuel mixture and accelerates the air–fuel homogenization. PM can play a vital role in improving the poor air–fuel mixing process and spray breakup characteristics of blended fuels with biodiesel; this is achieved by dispersing the fuel droplets and facilitating the proper space and time for air–fuel mixture formation.
3. PM application reduces the combustion pressure and temperature, which are crucial for emission control. It is mainly due to the heat absorption by the PM structure. The temperature and pressure decreased by 74% concerning the free spray of the GB10 case as the PM pore density increased to 20 PPI.
4. PM application increases the ignition delay time. The ignition delay time increase is more pronounced with an increase in the PM porosity, reaching 263% for the PM with a pore density of 20 PPI for GB0 free spray and 218% for GB5. Moreover, PM application lowers the peak heat release rate and extends the heat release duration, resembling homogeneous combustion.
5. The opposite effects of PM and biodiesel on combustion characteristics, including ignition delay, pressure rise, temperature rise, heat release rate, and fuel spray evolution in the gasoline compression ignition mode, can positively affect emissions, specifically those produced during the premixed and diffusion-controlled combustion

phases. Therefore, incorporating porous media in the combustion process of gasoline–biodiesel blended fuel can optimize air–fuel mixing and combustion characteristics.

Overall, this paper highlights the current study presented the benefits of biodiesel addition to gasoline and PM application for controlling gasoline combustion in GCI engines. Generally, the biodiesel addition increased the combustion peak pressure and temperature and reduced the ignition delay time and combustion duration, while the PM application had the opposite impact. However, this study had some potential limitations. The selection of natural gas for the preheating process resulted in high water vapor production, necessitating the total CVCC cleansing after each experiment. Substituting natural gas with other gases with less hydrogen in the molecular structure will expedite the experiments' performance.

Additionally, although a definite time was allocated for the homogeneity of the precombustion gases in the CVCC, the temperature inside the CVCC may not have been thoroughly homogenous. Performing the tests with a CVCC equipped with a mixer will create an ambient with a more homogenous temperature inside the CVCC and increase the results' repeatability. Considering the possible effects of the injector tip distance with the PM on the fuel spray formation and the ambient oxygen concentration (EGR ratio) on the combustion characteristics, future works must consider these factors as the probable tools to yield a more sophisticated strategy for combustion control. Moreover, an optical study of the blended fuel in the presence of PM combustion will provide more in-depth data on the spray formation and ignition delay of the blended fuel in the CVCC.

Acknowledgements The authors would like to thank the Iran Khodro Powertrain Company (IPCO) for providing the laboratory facility for this research.

Author contributions Mahdi Aboujafari helped in investigation, software, data curation, writing—original draft preparation. Mohammad Sadegh Valipour was involved in conceptualization, methodology, supervision and review and editing. Alireza Hajjalimohammadi contributed to methodology, project administration, supervision, writing—review and editing. Amir Hossein Parivar helped in resources, methodology.

Funding No funds, grants, or other support was received.

Data availability Data will be available upon request.

Declarations

Conflict of interest The authors declare that they have no conflict of interest.

References

- Reitz RD, Ogawa H, Payri R, Fansler T, Kokjohn S, Moriyoshi Y, et al. IJER editorial: the future of the internal combustion engine. *Int J Engine Res.* 2020;21:3–10.
- Kalghatgi GT, Risberg P, Ångström H-E. Advantages of fuels with high resistance to auto-ignition in late-injection, low-temperature, compression ignition combustion. *SAE trans.* 2006;623–634.
- Hu Y, Huang Z, Wang L, Sun X, Chen W. Experimental study on combustion and emissions of a compression ignition engine fueled with gasoline. *Adv Mech Eng.* 2022;14:168781322211099.
- Khoa NX, Putrasari Y, Vu DN, Duy NHX, Lim O. The effect of control strategies on the gasoline compression ignition (GCI) engine: injection strategy, exhaust residual gas strategy, biodiesel addition strategy, and oxygen content strategy. In: Kalghatgi G, Agarwal AK, Goyal H, Ben HM, editors. *Gasoline compression ignition technology: future prospects.* Springer: Singapore; 2022. p. 27–71. https://doi.org/10.1007/978-981-16-8735-8_3.
- Peng Q, Rockstroh T, Hall C. The impact of fuel and injection strategy on combustion characteristics, emissions and efficiency in gasoline compression ignition operation. *Fuel.* 2022;318:123548.
- Pratap Singh A, Kumar V, Kumar AA. Evaluation of reactivity controlled compression ignition mode combustion engine using mineral diesel/gasoline fuel pair. *Fuel.* 2021;301:120986.
- Jiang C, Li Z, Liu G, Qian Y, Lu X. Achieving high efficient gasoline compression ignition (GCI) combustion through the cooperative-control of fuel octane number and air intake conditions. *Fuel.* 2019;242:23–34.
- Jiang C, Huang G, Liu G, Qian Y, Lu X. Optimizing gasoline compression ignition engine performance and emissions: Combined effects of exhaust gas recirculation and fuel octane number. *Appl Therm Eng.* 2019;153:669–77.
- Bohlouli A, Mahdavian L. Catalysts used in biodiesel production: a review. *Biofuels.* 2021;12:885–98.
- Najafian A, Mahdavian L. Investigation of properties of biodiesel produced from sheep fatty wastes by eggshell. *Energy Environ Focus.* 2017;6:125–31.
- Widjaja G, Bohlouli A, Voronkova O, Mahdavian L. Investigation of thermodynamic parameters, combustion, and emissions of produced biodiesel fuel (from waste oil by heterogeneous nanocatalyst of stone cutting factory sludge) and its combination with diesel fuel. *J Therm Anal Calorim.* 2023;148:7781–93.
- Dalvand P, Mahdavian L. Calculation of the properties of biodiesel produced from castor seed by eggshell catalyst. *Biofuels.* 2018;9:705–10.
- Dalvand P, Mahdavian L. Biodiesel production in the presence of eggshell nano-catalyst. *Chem Technol Fuels Oils.* 2022;58:55–62.
- Ismaeel HKh, Albayati TM, Dhahad HA, Al-Sudani FT, Salih IK, Saady NMC, et al. Strategies for biodiesel production with the role of reactor technologies: a comprehensive review. *Chem Eng Process Process Intensif.* 2024;200:109767.
- Thongchai S, Kang Y, Lim O. A study of high-pressure gasoline spray added biodiesel 5% in a constant volume combustion chamber. *Energy Procedia.* 2019;158:607–11.
- Duy NHX, Lim O. A study on spray characteristic of gasoline-biodiesel blended under gci engines condition performed on constant volume combustion chamber system. *J Mech Sci Technol.* 2022;36:2095–106.
- Das SK, Jo H, Jwa KH, Lim O, Woo Y. Combustion characteristics of biodiesel blended gasoline fuel in engine like condition using constant volume combustion (CVCC). *Energy Procedia.* 2018;145:187–92.
- Vu DN, Lim O. Ignition and combustion characteristics of gasoline-biodiesel blend in a constant volume chamber: effects of the operation parameters. *Fuel.* 2019;255:115764.
- Zhong W, Li B, He Z, Xuan T, Lu P, Wang Q. Experimental study on spray and combustion of gasoline/hydrogenated catalytic biodiesel blends in a constant volume combustion chamber aimed for GCI engines. *Fuel.* 2019;253:129–38.
- Zhong W, Yuan Q, Liao J, Mahmoud Nasreldin M, Yuan W, He Z, et al. Experimental and modeling study of the autoignition characteristics of gasoline/hydrogenated catalytic biodiesel blends over low-to-intermediate temperature. *Fuel.* 2022;313:122919.
- Nam VD, Lim MT, Lim O. Study on auto-ignition characteristics of gasoline-biodiesel blend fuel in a rapid compression expansion machine. *Energy Procedia.* 2017;105:1789–95.
- Zare Ghadi A, Haghghi Asl A, Valipour MS. Numerical modeling of double-diffusive natural convection within an arc shaped enclosure filled with a porous medium. *J Heat Mass Transf Res.* 2014;1:83–91.
- Trimis D, Durst F. Combustion in a porous medium—advances and applications. *Combust Sci Technol.* 1996;121:153–68.
- Aboujafari M, Valipour MS, Hajjalimohammadi A, Honnery D. Porous medium applications in internal combustion engines: a review. *Transp Porous Media.* 2022;141:799–824.
- Banerjee A, Paul D. Developments and applications of porous medium combustion: a recent review. *Energy.* 2021;221:119868.
- Gharehghani A, Ghasemi K, Siavashi M, Mehranfar S. Applications of porous materials in combustion systems: a comprehensive and state-of-the-art review. *Fuel.* 2021;304:121411.
- Weclas M. Potential of porous-media combustion technology as applied to internal combustion engines. *J Thermodyn.* 2010;2010:1–39.
- Shahangian N, Ghojel J. The interaction between diesel sprays and porous media: effect of medium pore density and injection pressure. *J Porous Media.* 2012;15:501–16.
- Aggarwal H, Goel A, Kathpalia H, Kumar N. A study on homogeneous combustion in porous medium internal combustion engine: a review. *SAE Technical Paper 2017-01-0788*, 2017. <https://doi.org/10.4271/2017-01-0788>.
- Zhou L, Xie MZM, Luo KH. Numerical study of heat transfer and combustion in IC engine with a porous media piston region. *Appl Therm Eng.* 2014;65:597–604.
- Sharma D, Debnath BK. Computational investigation of porous media combustion technology in spark ignition engine. *Iran J Sci Technol Trans Mech Eng.* 2019;44:783–97.
- Liu HH, Xie MM, Wu D. Simulation of a porous medium (PM) engine using a two-zone combustion model. *Appl Therm Eng.* 2009;29:3189–97.
- Mohammadi A. Simulation of combustion in a porous-medium diesel engine. *Mech Sci Technol.* 2018;32:2327–37.
- Ali Ehyaei M, Tanehkar M, Rosen M. Analysis of an internal combustion engine using porous foams for thermal energy recovery. *Sustainability.* 2016;8:267.
- Cypris J, Schlier L, Travitzky N, Weclas M. Heat release process in three-dimensional macro-cellular SiC reactor under diesel engine-like conditions. *Fuel.* 2012;102:115–28.
- Tangestani V, Meghdadi Isfahani AH. Experimental evaluation of the performance and exhaust emissions of porous medium diesel and Otto engines. *Int J Environ Sci Technol.* 2020;17:1463–74.
- Saravanan S, Chidambaram RK, Geo VE. An experimental study to analyze influence of porous media combustor on performance and emission characteristics of a DI diesel engine. *Fuel.* 2020;280:118645.
- Das S, Debnath BK, Das RS. Analyzing the combustion behavior of different ceramic porous media in the piston bowl of a diesel engine. *J Inst Eng (India) Ser C.* 2022;103:573–87.
- Dong M, Xie M, Li S. Numerical study on turbulent two-phase flow in porous medium combustion chamber. *Sci China Ser E Technol Sci.* 2009;52:1511–20.

40. Zhao Z, Wang C, Xie M. Numerical study on the realization of compression ignition in a type of porous medium engine fueled with Isooctane. *Fuel*. 2009;88:2291–6.
41. Sohrabiasl I, Gorji-Bandpy M, Hajjalimohammadi A, Mirsalim MA. Effect of open cell metal porous media on evolution of high pressure diesel fuel spray. *Fuel*. 2017;206:133–44.
42. Shahangian N, Honnery D, Ghojel J. The role of porous media in homogenization of high pressure diesel fuel spray combustion. *J Energy Resour Technol*. 2014;136:012202.
43. Shahangian N, Honnery D, Ghojel J (2012) Homogenisation of high pressure diesel fuel spray combustion using porous ceramic media. In: ASME 2012 internal combustion engine division fall technical conference. American Society of Mechanical Engineers, pp 383–392
44. Saghaei M, Mohammadi A. Thermodynamic simulation of porous-medium combustion chamber under diesel engine-like conditions. *Appl Therm Eng*. 2019;153:306–15.
45. Azhdari Heravi A, Talebi F, Valipour MS. Investigation of pore-scale random porous media using lattice boltzmann method. *J Heat Mass Transf Res*. 2015;2:1–12.
46. Marasri S, Ewphun P-P, Srichai P, Charoenphonphanich C, Karin P, Tongroon M, et al. Combustion characteristics of hydrotreated vegetable oil-diesel blends under EGR and low temperature combustion conditions. *Int J Automot Technol*. 2019;20:569–78.
47. Holman JP. *Experimental methods for engineers*. 8th ed. New York: McGraw-Hill; 2012.
48. Das SK, Kim K, Lim O. Experimental study on non-vaporizing spray characteristics of biodiesel-blended gasoline fuel in a constant volume chamber. *Fuel Process Technol*. 2018;178:322–35.
49. Weclas M, Faltermeier R. Diesel jet impingement on small cylindrical obstacles for mixture homogenization by late injection strategy. *Int J Engine Res*. 2007;8:399–413.
50. Hajjalimohammadi A, Honnery D, Abdullah A, Mirsalim SM. Sensitivity analysis of parameters affecting image processing of high pressure gaseous jet images. *J Engine Res*. 2022;33:43–52.
51. Sun B, Zhao S, Zhai Y, Liu Q, Wu G, Wu H. Effect of fuel physicochemical properties on spray and particulate emissions. *ACS Omega*. 2022;7:44251–65.
52. Schönborn A, Ladommatos N, Williams J, Allan R, Rogerson J. The influence of molecular structure of fatty acid monoalkyl esters on diesel combustion. *Combust Flame*. 2009;156:1396–412.

Publisher's Note Springer Nature remains neutral with regard to jurisdictional claims in published maps and institutional affiliations.

Springer Nature or its licensor (e.g. a society or other partner) holds exclusive rights to this article under a publishing agreement with the author(s) or other rightsholder(s); author self-archiving of the accepted manuscript version of this article is solely governed by the terms of such publishing agreement and applicable law.